A Method for Quantitative Real-Time Evaluation of Measurement Reliability When Using Atomic Force Microscopy-Based Metrology

Abhijeet Gujrati, Subarna R. Khanal and Tevis D. B. Jacobs

***Abstract*—In atomic force microscopy (AFM) and metrology, it is known that the radius of the scanning tip affects the accuracy of the measurement. However, most techniques for ascertaining tip radius require interruption of the measurement technique to insert a reference standard or to otherwise image the tip. Here we propose an inline technique based on analysis of the power spectral density (PSD) of the topography that is being collected during measurement. By identifying and quantifying artifacts that are known to arise in the power spectrum due to tip blunting, the PSD itself can be used to determine progressive shifts in the radius of the tip. Specifically, using AFM images of an ultrananocrystalline diamond, various trends in measured PSD are demonstrated. First, using more than 200 different measurements of the same material, the variability in the measured PSD is demonstrated. Second, using progressive scans under the same conditions, a systematic shifting of the mid-to-high-frequency data is visible. Third, using three different PSDs, the changes in radii between them were quantitatively determined and compared to transmission electron microscopy (TEM) images of the tips taken immediately after use. The fractional changes in tip radii were detected; the absolute values of the tip radii could be matched between the two techniques, but only with careful selection of a fitting constant. Further work is required to determine the generalizability of the value of this constant. Overall, the proposed approach represents a step towards quantitative and inline determination of the radius of the scanning tip and thus of the reliability of AFM-based measurements.**

I. Introduction

Atomic force microscopy and metrology are widely used in the semiconductor industry to measure dimensions and surface roughness of substrates, films, and patterned features [1]. However, a significant limitation of AFM metrology is the shape of the tip [2]. Three problems emerge for a large-radius tip: (a) the accuracy of in-plane measurements is degraded due to the convolution of the tip with surface features; (b) height and depth measurements become inaccurate because the tip can no longer access the bottom of narrow trenches; and (c) surface roughness is incorrectly measured because the blunter tip cannot accurately sample fine-scale surface features [3]. The radius of the AFM tip can increase during measurement due to the build-up of contamination on the tip, or due to blunting caused by tip breakage or gradual sliding wear. Even more significantly, the degradation in resolution is not typically detected until the problem grows severe. Methods exist for assessing tip shape, including using electron microscopy to visualize the tip [4] and sliding the tip over a standard surface to enable numerical tip-reconstruction algorithms [5].

However, these approaches require interruptions in the metrology measurement and either a transition to a different substrate or the complete removal of the AFM tip. Here we present a method for the quantitative evaluation of tip radius that requires no interruption in metrology. Instead, using profile measurements that are already being collected on surfaces of interest, the power spectral density of the topography can be computed. By analyzing the random roughness that exists on most real-world surfaces, and specifically the loss of resolution of the fine-scale features in such roughness, changes in the tip radius can be detected in real-time.

II. Theoretical Background

The power spectral density is the Fourier transform of the autocorrelation function of the topography of a surface. Equivalently, it is defined as the square of the Fourier transform of the topography. It is used to mathematically decompose the overall topography into contributions from different spatial wavelengths λ, and is most often represented in frequency-space as a function of wavevector $q = 2\pi/\lambda$. For spatial information represented as an array of heights $h(x, y)$, the PSD can be computed and reported in various forms including a 2D representation $C^{2D}(q_x, q_y)$ [m^4], an isotropic 2D representation $C^{2D}(q_r)$ [m^3], and a 1D representation $C^{1D}(q_x)$ [m^3]. A full discussion of the differences between the various forms and their relationship to each other can be found in Ref. [3]. The present paper will exclusively use the one-sided, one-dimensional representation of the PSD, denoted as C^{1D+} [m^3], because this is the most common representation that is used for time-series data in the signal-processing literature.

Experimentally, the PSD is widely used to describe rough surfaces. The PSD of topography is often used qualitatively (for example, in Ref. [6]) to compare the relative spectral content of surface roughness between two surfaces. It is also used quantitatively, most often to extract self-affine (fractal-like) characteristics (for example, in Ref. [7]). For self-affine surfaces, the one-dimensional PSD can be fit with the expression

$$C^{1D}(q_x) = C_0 q_x^{-1-2H} \tag{1}$$

where C_0 is a constant and H is the Hurst exponent, which is related to the fractal dimension. More extensive quantitative

*Research supported by the Central Research Development Fund program at the University of Pittsburgh.

Abhijeet Gujrati, Subarna R. Khanal, and Tevis D.B. Jacobs are with the Department of Mechanical Engineering and Materials Science, University of Pittsburgh, Pittsburgh, PA, USA. (phone: 412-624-9736; e-mail: abg30@pitt.edu ; tjacobs@pitt.edu).

use of experimentally-measured PSDs (for instance, for properties prediction) has been limited, primarily due to the limitations discussed in Ref. [3]. Here one of these inherent limitations will be exploited to approximate the radius of the scanning tip.

The tip radius determines the minimum length scale (i.e. the maximum wavevector q) that can be accurately measured [8-10]. For a sinusoidal surface, the minimum wavelength λ_c that can be sampled by a spherical-ended tip of radius R_{tip} is given by [11]:

$$\lambda_c = 2\pi\sqrt{\chi R_{tip}} \tag{2}$$

where χ is the amplitude of the sine wave. According to Church and Takacs [11-13], the finite size of the tip leads to an asymptotic decay of the measured power spectrum, which follows a predictable form. For the one-dimensional PSD, this is given by [11]:

$$C^{1D}(q_x) = \frac{c}{\pi} q_x^{-4} \tag{3}$$

where c is a constant of order unity. This artifacted topography should appear linear on a log-log plot, and thus appear to be self-affine. However, the artifacted topography should yield *H=1.5*, which is outside the range of what is typically observed for surfaces [14]. Therefore, this artifacted topography should be distinguishable from the underlying true topography, in the form of a change in slope.

More specifically, this transition from accurate topography to artifacted topography should occur at a certain cutoff frequency q_c, which can be defined [3] as the point where the radius of curvature of the tip equals the root-mean-square curvature h''_{rms} of the surface. That is:

$$h''_{rms}(q_c) \approx {}^{c}/_{R_{tip}} \tag{4}$$

Following Parseval's theorem, the root-mean-square parameters of the surface can be computed from the one-sided, one-dimensional PSD of the surface topography. Specifically:

$$(h_{rms})^2 = \frac{1}{\pi}\int_0^\infty C^{1D+}(q_x)dq_x \tag{5a}$$

$$\left(h'_{rms}\right)^2 = \frac{1}{\pi}\int_0^\infty q_x^2 C^{1D+}(q_x)dq_x \tag{5b}$$

$$\left(h''_{rms}\right)^2 = \frac{1}{\pi}\int_0^\infty q_x^4 C^{1D+}(q_x)dq_x \tag{5c}$$

Therefore, the principle of the given method is to use the PSD first to identify the transition point in slope (which gives the value of q_c), and second to compute the fourth moment of the PSD over the interval $q = [0; q_c]$. This yields the left-hand-side of Eq. 4. By observing this value over time, changes in tip radius can be detected among multiple scans of a similar surface. Alternatively, by assuming a particular value of c, then the absolute value of tip radius can be approximated.

The present method is distinct from the one proposed by Knoll [15]. That analysis, which works for soft polymer films, assumes complete contact at the size scale of the contact radius. By contrast, the present approach, which works for harder materials, assumes incomplete contact of the blunt tip with the rough surface. These two analyses lead to different functional forms of the PSD, with different fitting and analysis.

Overall, the present approach for hard materials is well-suited to the semiconductor industry and can be used to detect real-time changes in tip radius – even before they become so severe as to be noticeable to the user.

III. Experimental Methods

The use of this method was investigated by scanning the topography of a surface of ultrananocrystalline diamond (UNCD) (Advanced Diamond Technology, Romeoville, IL). First, in order to identify the range of PSD measurements that are possible for the same surface, the topography of the UNCD was measured in tapping mode using 203 different individual scans. These were performed on three different machines (Bruker Dimension, Asylum Cypher, and Asylum MFP-3D), with silicon and diamond-like carbon (DLC)-coated tips (NCLR, NCHR, CONTR, Tap DLC 300), and with scan sizes ranging from 100 nm to 100 μm. The free-air amplitudes and amplitude ratios were varied over the range from 37-73 nm and 0.40-0.15, respectively, in order to intentionally vary the surface stresses, which should alter the amount of tip wear [13]. The measured surface was collected for every scan and used to compute [3] the PSD by: tilt-compensating each line of the image the image; applying a sum-preserving windowing function; and numerically computing the square of the Fourier transform for each line scan in the fast-scan direction. Individual lines from a single scan were averaged to yield the 1D PSD.

Second, to demonstrate the systematic nature of the decay of the PSD, one AFM tip was used to sequentially measure the same surface to look for systematic changes in the PSD. Seventeen scans were collected using a silicon probe (NCHR) over a scan size of 2 μm with a free air amplitude of 49 nm and an amplitude ratio of 0.5.

Third, three of the AFM tips from the initial 203 scans were imaged using a transmission electron microscope to measure their radii and compare to values computed from the PSD. To measure the radius in the TEM, the tips were imaged at 200 keV using a JEOL 2100F with a probe-holder fixture [4]. Using image analysis, the outer profile was extracted and fit to a parabola of the form $z = r^2/2R_{tip}$, to extract the best-fit radius. To measure the radius using the PSD (via the approach outlined in the previous section), four steps were implemented. First, the electronic noise in the images was subtracted out. To do this, a noise spectrum was measured under identical circumstances to the topography measurement, but with lateral scanning disabled. In all cases, the noise data could be fit $C_{noise}(q_x) = C_{0,noise} q_x^{-1}$, which is equivalent to an apparent Hurst exponent of zero, and

which is often called pink noise in the signal processing community. Because ambient conditions can change with time, the value of $C_{0,\,noise}$ was adjusted to match the final data point of each spectrum. In this way, the instantaneous noise spectrum was subtracted from the measured spectrum. Second, the transition point in slope was identified by fitting the left-most side of the PSD using a self-affine line, and then looking for deviation from that scaling. The transition is not sharp, but can often be identified. Further, in comparing two different measurements, it can be more obvious. This transition point defines the cutoff frequency q_c for reliable region. Third, the root-mean-square curvature was evaluated up to q_c using Eq. 5c. Fourth, the tip radius was evaluated using Eqs. 5c and 4.

IV. Results And Discussions

An example PSD of the topography from a tip-artifacted AFM measurement is shown in Fig. 1. Three regimes are apparent in this figure. The low-frequency data, where the tip is accurately sampling the surface, is assumed to represent the true underlying topography. The Hurst exponent can be recovered from the low-frequency regime, and indeed similar scaling behavior has been confirmed at larger length scales using stylus profilometry. There is a transition to a steeper-slope region where the PSD scales as q^{-4}; this is assumed to be the tip-artifacted regime discussed in the previous section. Finally, the PSD rolls upward at the highest frequencies, which represents noise in the measurement system. The PSD of a typical noise scan, with lateral motion disabled, is also shown in Fig. 1.

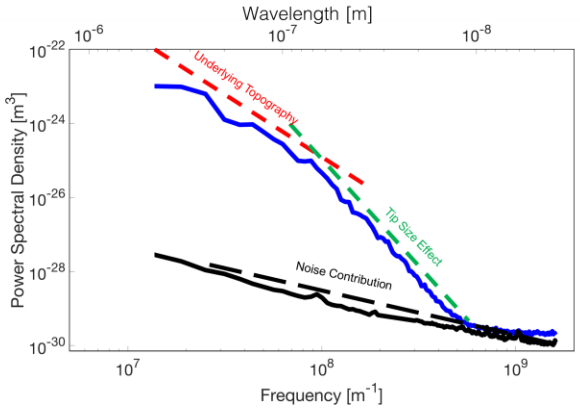

Figure 1. A sample power spectral density (blue, solid) from a tip-artifacted AFM measurement shows three regions: the low-frequency (long-wavelength) region most likely represents the true topography; the middle region represents the tip-artifacted topography; and the high-frequency (short-wavelength) region shows an upward curve due to the contribution of noise. Dashed lines are used to guide the eye for each region. For reference, the solid black line represents a noise-characterization measurement where the lateral scanning was turned off.

In Fig. 2, the PSDs from 203 individual measurements of UNCD shows the wide variation in results that are possible with repeated measurements. These measurements were taken in different locations on the UNCD substrate, but the material is known to show consistent topography and is extremely wear-resistant. The variability in measurement is instead attributed to variations in tip condition.

To examine the effects on a single tip, 14 scans were taken sequentially using the same Si tip on the same UNCD surface. As shown in Fig. 3, there is a distinct change in slope between the underlying topography and tip artifacted regime. The location of this transition varies from one scan to another.

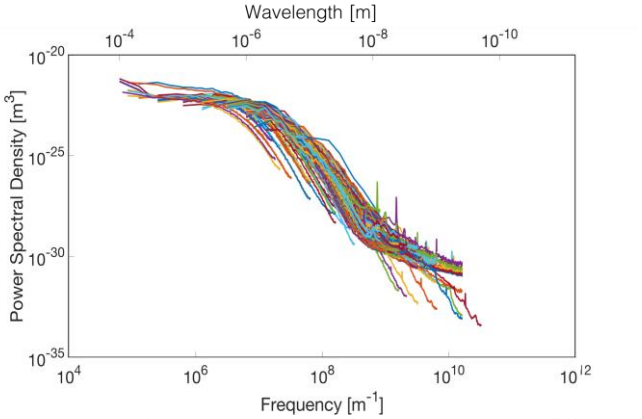

Figure 2. More than 200 AFM scans of the same surface under different conditions and with different tips demonstrates the variability that is possible in the measured PSD of a surface. At the lowest frequencies, a flattening is observed that is not represented in Fig. 1; this represents "roll-off" of the long-wavelength topography [14].

This variation is attributed to progressive tip wear and blunting, which causes a reduction in C^{ID} at large values of q_c. In the context of Eq. 4, this corresponds to a decrease in both sides of the equation. Because the slope of the artifacted region is the same, then a decrease in q_c manifests as a series of parallel lines with progressively leftward-shifting locations.

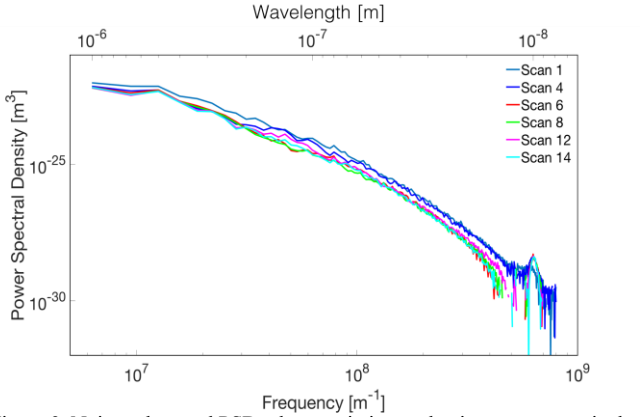

Figure 3. Noise-subtracted PSDs show variation as the tip gets progressively blunter. In particular, while the low-frequency data stays approximately constant, the high-frequency portion of the curve appears to shift progressively leftward. This corresponds to a leftward shift in the transition point between true and artifacted topography.

Finally, this present quantitative PSD analysis technique has been performed for 3 AFM scans with 3 different tips where the tip radius was explicitly measured via TEM immediately after use, as shown in Fig. 4. A systematic trend was observed, where the integration of h''_{rms} up to q_c (i.e. the value of c/R_{tip}) decreased from 19.5 to 14.5 to 1.42 μm^{-1}. This represents a difference of 18.8% between the highest and second-highest values, and a fourteen-fold difference between the highest and lowest values. The TEM images demonstrated that the three imaged tips had radii of 13, 17, and 115 nm, which correspond to an 23.5% difference

between the highest and second-highest values, and a nine-fold difference between the highest and lowest values. This indicates that the trends in behavior are well reflected in this case. To extract absolute values of R_{tip} requires an assumption about the value of c. Further investigation is required to understand the correct value of c to be applied. In this case, a value of $c = 0.2$ leads to radii of 10.2, 13.8, and 140.5 nm, which match the TEM measurements reasonably well. However, it is not yet clear how reproducible that trend is and thus how universal this value of c should be considered.

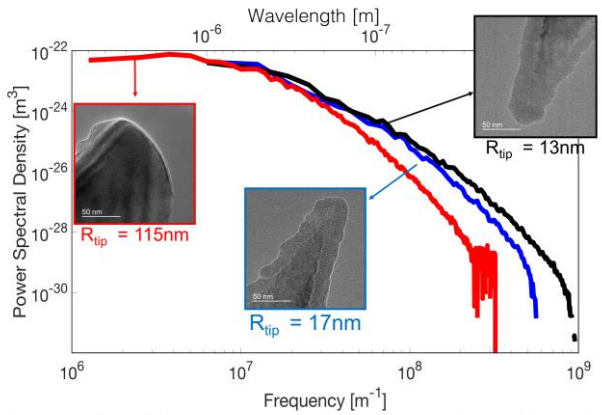

Figure 4. Three different AFM scans from Fig. 2 are featured here, along with the TEM images of the AFM tips used to measure them. The TEM-measured profile of the apex was fit to determine the tip radius shown. The variations in the PSD, including a leftward-shifting transition point, are readily apparent. As discussed in the main text, the present method is able to accurately capture the increase in the tip radius. With careful selection of the constant c, the absolute values of the radii can be reproduced reasonably, but further work is required to determine the generalizability of this choice of c.

These results show: (i) meaningful differences in PSD measurements, which are attributed primarily to variations in tip geometry; and (ii) that the present approach captures trends in tip radius that are seen using direct imaging with TEM. The most significant source of error in the calculations is the determination of the cutoff frequency, which does not always show a sharp transition from one slope to another. This can be partially mitigated by looking at the leftward shift in the artifacted region of the PSD for multiple measurements taken with the same tip under similar conditions. By fitting these with straight lines and extrapolating back to the best-fit line of topography, the cutoff frequency can be chosen as the point of their crossing.

V. Conclusion

Here we have shown the importance of accurate knowledge of the AFM tip radius, and also the variation in PSD that can be measured when the radius is not accounted for. An inline technique has been proposed for assessing the reliable region of AFM-based metrology measurements, and for detecting changes in tip radius over time. The approach is demonstrated and, in three different cases, correlates with tip radius measurements taken using direct imaging in the TEM.

Acknowledgment

This work was funded by the Central Research Development Fund at the University of Pittsburgh. We thank Dr. Lars Pastewka for helpful discussion. Use of the Nanoscale Fabrication & Characterization Facility in the Petersen Institute of NanoScience and Engineering at the University of Pittsburgh is acknowledged.

References

[1] R. G. Dixson, R. G. Koening, J. Fu, T. V Vorburger, and B. T. Renegar, "Accurate dimensional metrology with atomic force microscopy," in *Microlithography 2000*, 2000, pp. 362–368.

[2] W. Häßler-Grohne, D. Hüser, K.-P. Johnsen, C. G. Frase, and H. Bosse, "Current limitations of SEM and AFM metrology for the characterization of 3D nanostructures," *Meas. Sci. Technol.*, vol. 22, no. 9, p. 94003, 2011.

[3] T. D. B. Jacobs, T. Junge, and L. Pastewka, "Quantitative characterization of surface topography using spectral analysis," *Surf. Topogr. Metrol. Prop.*, vol. 5, no. 1, p. 13001, 2017.

[4] T. D. B. Jacobs, G. E. Wabiszewski, A. J. Goodman, and R. W. Carpick, "Characterizing nanoscale scanning probes using electron microscopy: A novel fixture and a practical guide," *Rev. Sci. Instrum.*, vol. 87, no. 1, p. 13703, 2016.

[5] J. S. Villarrubia, "Morphological estimation of tip geometry for scanned probe microscopy," *Surf. Sci.*, vol. 321, no. 3, pp. 287–300, 1994.

[6] D. H. Alsem, H. Xiang, R. O. Ritchie, and K. Komvopoulos, "Sidewall adhesion and sliding contact behavior of polycrystalline silicon microdevices operated in high vacuum," *J. Microelectromechanical Syst.*, vol. 21, no. 2, pp. 359–369, 2012.

[7] S. Patra, S. Sarkar, S. K. Bera, G. K. Paul, and R. Ghosh, "Influence of surface topography and chemical structure on wettability of electrodeposited ZnO thin films," *J. Appl. Phys.*, vol. 108, no. 8, p. 83507, 2010.

[8] K. L. Westra and D. J. Thomson, "Effect of tip shape on surface roughness measurements from atomic force microscopy images of thin films," *J. Vac. Sci. Technol. B Microelectron. Nanom. Struct. Process. Meas. Phenom.*, vol. 13, no. 2, pp. 344–349, 1995.

[9] K. A. O'Donnell, "Effects of finite stylus width in surface contact profilometry," *Appl. Opt.*, vol. 32, no. 25, pp. 4922–4928, 1993.

[10] D. L. Sedin and K. L. Rowlen, "Influence of tip size on AFM roughness measurements," *Appl. Surf. Sci.*, vol. 182, no. 1, pp. 40–48, 2001.

[11] E. L. Church and P. Z. Takacs, "Effects of the nonvanishing tip size in mechanical profile measurements," in *San Dieg-DL Tentative*, 1991, pp. 504–514.

[12] E. L. Church and P. Z. Takacs, "Instrumental effects in surface finish measurement," in *1988 International Congress on Optical Science and Engineering*, 1989, pp. 46–55.

[13] R. Leach, A. Weckenmann, J. Coupland, and W. Hartmann, "Interpreting the probe-surface interaction of surface measuring instruments, or what is a surface?," *Surf. Topogr. Metrol. Prop.*, vol. 2, no. 3, p. 35001, 2014.

[14] B. N. J. Persson, "On the fractal dimension of rough surfaces," *Tribol. Lett.*, vol. 54, no. 1, pp. 99–106, 2014.

[15] A. W. Knoll, "Nanoscale contact-radius determination by spectral analysis of polymer roughness images," *Langmuir*, vol. 29, no. 45, pp. 13958–13966, 2013.